Since January 2020 Elsevier has created a COVID-19 resource centre with free information in English and Mandarin on the novel coronavirus COVID-19. The COVID-19 resource centre is hosted on Elsevier Connect, the company's public news and information website.

Virus Research 176 (2013) 265–272

Contents lists available at ScienceDirect

Virus Research

journal homepage: www.elsevier.com/locate/virusres

A study of the virulence in mice of high copying fidelity variants of human enterovirus 71

Sara Sadeghipour, Peter C. McMinn*

Infectious Diseases and Immunology, Sydney Medical School, Blackburn Building D06, The University of Sydney, NSW 2006, Australia

ARTICLE INFO

Article history:
Received 17 May 2013
Received in revised form 26 June 2013
Accepted 26 June 2013
Available online 12 July 2013

ABSTRACT

Polioviruses with a G64S mutation in the 3D polymerase have enhanced replication fidelity and are attenuated in animal models. Here we describe the mouse virulence properties of high replication fidelity 3D polymerase variants of human enterovirus 71 (HEV71), with mutations at positions 3D-S264L, 3D-G64R or at 3D-S264L plus 3D-G64R. Mouse-adapted strains (MP-G64R, MP-S264L and MP-S264L-G64R) were constructed in order to compare the virulence of the 3D polymerase variants with that of mouse-adapted parental virus (MP-26M). MP-S264L and MP-S264L-G64R were attenuated in mice (mean survival time 7.0 and 7.5 days p.i., respectively) compared to MP-G64R and MP-26M (mean survival time 6.5 and 6.0 days p.i., respectively). MP-26M and MP-G64R infection induced early onset, severe generalised necrotising myositis, whereas MP-S264L and MP-S264L-G64R infection induced a later onset, mild and focal skeletal muscle myositis. Our findings demonstrate that only the 3D-S264L mutation attenuates HEV71 in mice, suggesting that the high replication fidelity phenotype is not essential for virulence attenuation in this model.

1. Introduction

Human enterovirus 71 (HEV71) belongs to the genus *Enterovirus* within the family *Picornaviridae* (Knowles et al., 2012). HEV71 was first discovered in 1969 and has recently emerged as an important cause of hand-foot-and-mouse disease (HFMD) associated with a high frequency of acute neurological disease (McMinn, 2002).

The poliovirus 3D polymerase ($3D^{pol}$) has recently gained attention as a promising virulence attenuation target (Pfeiffer and Kirkegaard, 2003; Vignuzzi et al., 2008). A poliovirus variant with a G64S mutation in the $3D^{pol}$ coding region has been shown to express high replication fidelity and to be attenuated in poliovirus receptor-expressing transgenic mice (Pfeiffer and Kirkegaard, 2005; Vignuzzi et al., 2006, 2008). Furthermore, G64A, G64T, G64L and G64V mutations in the poliovirus $3D^{pol}$ have been shown to greatly reduce viral fitness and to attenuate virulence (Vignuzzi et al., 2008). Attenuating mutations that increase the replication fidelity of the poliovirus $3D^{pol}$ have also been shown to prevent reversion to virulence of the parental virus phenotype (Pfeiffer and Kirkegaard, 2005; Vignuzzi et al., 2008). Furthermore, we have recently identified two mutations in HEV71 $3D^{pol}$, at positions G64R and S264L, that increase replication fidelity during growth in cell culture (Sadeghipour et al., 2013).

In this study, we examine the relationship between $3D^{pol}$ mutations (G64R, S264L) that confer a high replication fidelity phenotype upon HEV71 and their virulence phenotype in mice. We investigate the virulence of HEV71 strains containing $3D^{pol}$ mutations at positions G64R, S264L and at S264L plus G64R (double mutant) in a newborn BALB/c mouse model of HEV71 infection (Chua et al., 2008). 50% humane endpoints, mean lengths of survival, viral distribution in mouse tissues and histological studies were undertaken in order to compare the virulence of the HEV71 $3D^{pol}$ variants with that of virulent parental virus.

2. Materials and methods

2.1. Virus, cell lines and media

HEV71 strain 26M/AUS/4/99, sub-genotype B3, was isolated in Western Australia in 1999 (Chua et al., 2008; McMinn et al., 2001) during an outbreak of hand, foot and mouth disease. HEV71-26M has been fully sequenced and used to generate an infectious cDNA clone (Chua et al., 2008). MP-26M is a mouse-adapted strain (VP1-G145E) of HEV71-26M (Chua et al., 2008). Human rhabdomyosarcoma (RD; ATCC number CCL-136), African green monkey kidney (Vero; ATCC number CCL-81) and simian virus 40-transfected African green monkey kidney (COS-7; CRL-1651) cell lines were maintained at 37 °C in 5% CO_2. Maintenance medium

* Corresponding author. Tel.: +61 2 9351 2900; fax: +61 2 9351 4731.
E-mail address: peter.mcminn@sydney.edu.au (P.C. McMinn).

0168-1702/$ – see front matter © 2013 Elsevier B.V. All rights reserved.
http://dx.doi.org/10.1016/j.virusres.2013.06.019

was Dulbecco's Modified Eagle Medium (DMEM) (HyClone) supplemented with 2% foetal bovine serum (FBS) (Bovogen Biologicals) and 2 mM L-glutamine (Sigma). Growth medium was DMEM supplemented with 5% FBS and 2 mM L-glutamine.

2.2. Cloning

In order to select HEV71 strains with high replication fidelity, the 3D-G64R (Sadeghipour et al., 2013), 3D-S264L (Sadeghipour et al., 2013) and 3D-S264L-G64R mutations were introduced into pcDNA3-3D by site-directed mutagenesis using the Lightning Quickchange mutagenesis kit (Stratagene). The 3D coding region fragments carrying the G64R, S264L or S264L-G64R mutations were cloned into the HEV71-26M infectious cDNA clone by digestion with *Mlu*I and *Eco*RV to produce G64R (Sadeghipour et al., 2013), S264L (Sadeghipour et al., 2013) and S264L-G64R, respectively. The 3D gene fragments carrying the 3D-G64R, 3D-S264L or 3D-S264L-G64R mutations were also cloned into the mouse-adapted MP-26M infectious cDNA clone by digestion with *Mlu*I and *Eco*RV to generate MP-G64R, MP-S264L and MP-S264L-G64R, respectively.

2.3. Transfection

Recombinant full-length HEV71 plasmids were transfected into COS-7 cells using Lipofectamine 2000 (Invitrogen) to rescue clone-derived virus (CDV). Briefly, 1.6 μg of either G64R, S264L or S264L-G64R and 1.6 μg pCMVT7-Pol expressing the T7 RNA polymerase were diluted into a final volume of 100 μL containing 4 μL Lipofectamine 2000 in 96 μL OptiMEM (Invitrogen). The two solutions were incubated for 5 min, then combined and incubated for a further 20 min at room temperature. COS-7 cells in 12-well tissue culture plates (CellStar) were covered with 400 μL of the OptiMEM solution. After 4 h incubation at 37 °C, 600 μL of growth medium was added and the transfected cells were incubated for 72 h. Transfected cells were then subjected to three cycles of freeze-thawing and the supernatants clarified by centrifugation at 6500 × *g* for 5 min; 200 μL of transfected COS-7 cell lysate was used to infect RD cells in six-well plates. CDVs were passaged (×1) on RD cells to obtain working stocks. CDV-infected cell culture supernatants were subjected to viral RNA extraction using the QIAamp viral RNA minikit (Qiagen) and viral cDNA synthesis was performed using Superscript III (Invitrogen) and the 3′-UTR-R primer. Viral cDNA was amplified by polymerase chain reaction (PCR) followed by nucleotide sequencing of the 3D coding region to confirm the presence of the 3D-G64R, 3D-S264L or 3D-S264L-G64R mutations or the VP1 coding region to confirm the presence of the VP1-G145E mouse adaptation marker.

2.4. Characterisation of the S264L-G64R double mutant

2.4.1. Investigation of the ribavirin resistance phenotype

The growth of S264L-G64R was compared to parental 26M in RD cell culture for 24 h in the presence of 0 μM, 800 μM or 1600 μM ribavirin. Briefly, RD cells in 12-well plates (Cellstar) were covered with DMEM containing 0 μM, 800 μM or 1600 μM ribavirin for 1 h at 37 °C. The ribavirin-pre-treated RD cells were washed once with phosphate-buffered saline, pH 7.4 (PBS). Cells were infected (MOI = 0.1) with parental 26M or S264L-G64R for 1 h at 37 °C, washed with PBS, followed by the addition of maintenance medium containing either 0 μM, 800 μM or 1600 μM ribavirin. The infected cell cultures were then incubated at 37 °C in 5% CO_2 for 24 h. At the conclusion of the experiment, virus was released from cells by freeze-thawing (×3) and the lysate was clarified by centrifugation at 6500 × *g* for 5 min. The titre of the lysate was determined by $TCID_{50}$ assay on Vero cells, following Reed and Muench (Reed and Muench, 1938).

2.4.2. Plaque purification of S264L-G64R

Twelve-well tissue culture trays (Cellstar) were seeded with Vero cells at a density of 2.2×10^5 cells/well and grown overnight at 37 °C. Ten-fold serial dilutions of virus were inoculated onto Vero cell monolayers at a volume of 200 μL per well. After incubation for 30 min at 37 °C, virus was removed and cells were washed with PBS. Cells were then overlaid with 1 mL of maintenance medium containing 0.5% immunodiffusion-grade agarose (ICN) and incubated at 37 °C in 5% CO_2. After four days incubation, an additional 0.5 mL of maintenance medium containing 0.5% immunodiffusion-grade agarose was added to each well and the cultures incubated for a further three days. Isolated plaques were selected using a pipette tip to draw up the cells from within the plaque. This protocol was repeated three times in order to select plaque-purified virus populations.

2.4.3. Characterisation of the guanidine sensitivity of plaque-purified populations of S264L-G64R during passage in RD cells in the presence of ribavirin

The guanidine sensitivities of plaque-purified populations of S264L-G64R were compared to plaque-purified populations of parental 26M by growth in the presence of either 0 mM or 0.5 mM guanidine for 48 h. Briefly, RD cells were infected (MOI = 0.1) in six-well plates (Cellstar) for 1 h at 37 °C. Cells were washed with PBS and maintenance medium containing either 0 mM or 0.5 mM guanidine was added. Cells were incubated at 37 °C in 5% CO_2 for 48 h. Virus was released from cells by freeze-thawing (×3) and the lysate was clarified by centrifugation at 6500 × *g* for 5 min. The titre of the lysate was determined by $TCID_{50}$ assay, as described above (Reed and Muench, 1938).

2.4.4. RNA extraction, cDNA synthesis and nucleotide sequence analysis

Viral RNA was extracted from parental 26M and S264L-G64R after one or thirteen passages in RD cells in the presence of ribavirin (400 μM), using the QIAamp Viral RNA Mini Kit (Qiagen); 8 μL of viral RNA was reverse transcribed using Superscript III (Invitrogen) and the 3′-UTR-R primer. Viral cDNA was amplified by PCR and gel-purified using a MinElute gel extraction kit (Qiagen). Nucleotide sequencing of coding regions 2C and 3D was performed by the Australian Genome Research Facility. Analysis of DNA chromatograms were performed using the program Chromas™ version 2.33 (Technelysium Pty. Ltd. Australia) and Sequencher version 4.7 (Gen Codes Corporation). Statistical analyses were performed using two-tailed Student's *t*-test; *P* values of <0.05 are considered statistically significant.

2.4.5. Single-step growth kinetics

RD cell monolayers (1×10^5 cells per well) grown overnight in 48-well tissue culture plates (Cellstar) were infected (MOI = 10) for 1 h at 37 °C. Cells were then washed with PBS (×3) and overlaid with 300 μL of maintenance medium per well. Virus was collected at four hourly intervals for 24 h by freeze-thawing (×3) and clarified by centrifugation at 6500 × *g* for 5 min. The first time point (0 h) was collected immediately after the addition of the maintenance medium. Yields were quantified by $TCID_{50}$ assay, as described above (Reed and Muench, 1938).

2.5. Determination of HD_{50} values

In order to minimise distress to the experimental animals, 50% humane endpoints (HD_{50}) were used instead of 50% lethal endpoints (LD_{50}); humane endpoint assays have been shown to be

statistically identical to lethal end-point virulence assays (Wright and Phillpotts, 1998).

Groups of six 5-day-old BALB/c mice were infected by intraperitoneal (i.p.) inoculation with 50 μL of ten-fold serial dilutions of MP-26M, MP-G64R, MP-S264L or MP-S264L-G64R. Mock-infected mice were inoculated with diluent (DMEM) only and monitored for clinical signs of infection for 14 days. Mice that developed grade 3 paralysis (hunched posture, flaccid paralysis) were euthanised. The HD_{50} value in 5-day-old BALB/c mice was calculated using the method of Reed and Muench (Reed and Muench, 1938).

2.6. Survival analysis

Groups of six 5-day-old BALB/c mice were infected i.p. with 50 μL DMEM containing 5×10^0, 5×10^1, 5×10^2, 5×10^3 or 5×10^4 $TCID_{50}$ of MP-26M, MP-G64R, MP-S264L or MP-S264L-G64R. Mock-infected mice were inoculated with diluent (DMEM). Mice were monitored twice daily for 14 days p.i. and the percentage survival calculated for each group; mice showing grade 3 paralysis or greater were euthanised. Statistical analyses were performed using Mantel–Cox Log-rank test; P values of <0.05 are considered statistically significant.

2.7. Tissue distribution and viral load determination

Groups of five-day-old BALB/c mice were infected i.p. with $50 \times HD_{50}$ of MP-26M, MP-G64R, MP-S264L or MP-S264L-G64R. At the indicated times p.i., three mice from each group were euthanised by i.p. injection with a mixture of xylazine (20 mg mL^{-1}) and ketamine (100 mg mL^{-1}) in PBS at a dose of 5 μL/g body $weight^{-1}$. Whole blood was collected by intracardiac puncture and stored at −80 °C. After perfusion with PBS, tissue samples were collected, weighed individually, snap-frozen in liquid nitrogen and stored at 80 °C. Tissues were homogenised with a Dounce homogeniser and the homogenates prepared as 10% (w/v) suspensions in Hanks' balanced salt solution, pH 8.0 (HBSS). Virus titres in each tissue homogenate were determined by $TCID_{50}$ assay on Vero cells. Viral titres in blood were determined as $TCID_{50}$ mL^{-1}; viral titres in tissue homogenates were determined as $TCID_{50}$ g^{-1}.

2.8. Histological studies

Skeletal muscle tissue for histological analysis was collected from three infected mice demonstrating clinical signs of HEV71 infection of grade 3 or greater, fixed in 10% buffered formalin overnight, dehydrated in 70% ethanol and embedded in paraffin. For each tissue specimen, several sections (4–5 μm) were cut with a microtome, mounted onto glass slides (VWR Labware) and stained with haematoxylin and eosin.

2.9. Statistical methods

Statistical analyses were performed using one-way ANOVA and Tukey's multiple comparison tests, the Mantel–Cox Log-rank test or the two-tailed Student's t-test. P values of <0.05 are considered statistically significant. Data were analysed using the GraphPad Prism online software package.

3. Results

We have previously shown that the mutations 3D-G64R and 3D-S264L confer ribavirin resistance upon HEV71 by increasing the replication fidelity of $3D^{pol}$ (Sadeghipour et al., 2013). Furthermore, it has been shown that amino acid substitutions at position G64 in the poliovirus $3D^{pol}$ not only induce resistance to ribavirin and increase replication fidelity but also lead to reduced virulence in poliovirus receptor-expressing transgenic mice (Pfeiffer and Kirkegaard, 2003, 2005; Vignuzzi et al., 2006, 2008). Thus, we were interested to determine if the HEV71 $3D^{pol}$ mutations are also able to attenuate viral virulence in a mouse model of HEV71 infection (Chua et al., 2008).

3.1. Construction and expression of a cloned population of the S264L-G64R double mutant

In order to select HEV71 strains with high replication fidelity and stable attenuation of virulence, a double mutant strain incorporating both 3D-S264L and 3D-G64R was constructed by site-directed mutagenesis of the HEV71 infectious cDNA clone (Chua et al., 2008), generating the variant S264L-G64R. CDVs were passaged ten times in RD cells to assess the stability of the introduced mutations during passage in cell culture. Both the 3D-S264L and 3D-G64R mutations remained stably present through ten passages of the double mutant CDV in RD cells (data not shown). As a first step in characterising the phenotype of S264L-G64R, we determined its ribavirin resistance and RNA copying fidelity phenotypes.

3.2. Characterisation of the ribavirin resistance phenotype of S264L-G64R in RD cell culture

We have previously shown that the 3D-G64R and 3D-S264L mutations are responsible for the ribavirin-resistant phenotype of HEV71 (Sadeghipour et al., 2013). In order to examine the susceptibility of the double mutant CDV population to ribavirin, S264L-G64R and parental 26M were grown in RD cells for 24 h in the presence or absence of 800 μM or 1600 μM ribavirin, respectively. The results of this experiment are shown in Fig. 1A and the ratio of the RD cell growth titres of the parental and variant CDV populations in the presence or absence of ribavirin is shown in Fig. 1B. As expected, S264L-G64R was capable of growth in the presence of 1600 μM ribavirin (4.8×10^5 $TCID_{50}$/mL), at only a 2-fold lower titre than that in absence of ribavirin (1.0×10^6 $TCID_{50}$/mL). By contrast, the growth of parental 26M was strongly inhibited in the presence of 800 μM ribavirin (5.4×10^4 $TCID_{50}$/mL) at a titre approximately 50-fold below the growth titre in the absence of ribavirin (2.5×10^6 $TCID_{50}$/mL). As expected, these experiments confirm that S264L-G64R is resistant to growth in the presence of ribavirin, as we previously observed in CDVs incorporating the single $3D^{pol}$ mutations (Sadeghipour et al., 2013).

3.3. Single-step growth kinetics of the S264L-G64R

We have previously shown that the 3D-G64R and 3D-S264L mutations do not impact significantly on the growth of the G64R and S264L CDV populations in RD cells (Sadeghipour et al., 2013). Single-step growth kinetic studies were performed in order to determine if the higher titre growth of the S264L-G64R polymerase variants in RD cells in the presence of ribavirin compared to parental virus was due either wholly or partly to increased replicative capacity. RD cells were infected (MOI = 10) and virus growth was measured over a 24 h time course. The growth kinetics in RD cells of S264L-G64R was compared to parental virus (Fig. 2). In the absence of ribavirin pressure, S264L-G64R and parental virus populations grew efficiently in RD cells with no statistically significant differences ($P > 0.05$) observed in their single-step growth kinetics (Fig. 2). Thus, the 3D-S264L-G64R mutation does not impact significantly on the growth of the S264L-G64R CDV population in RD cells.

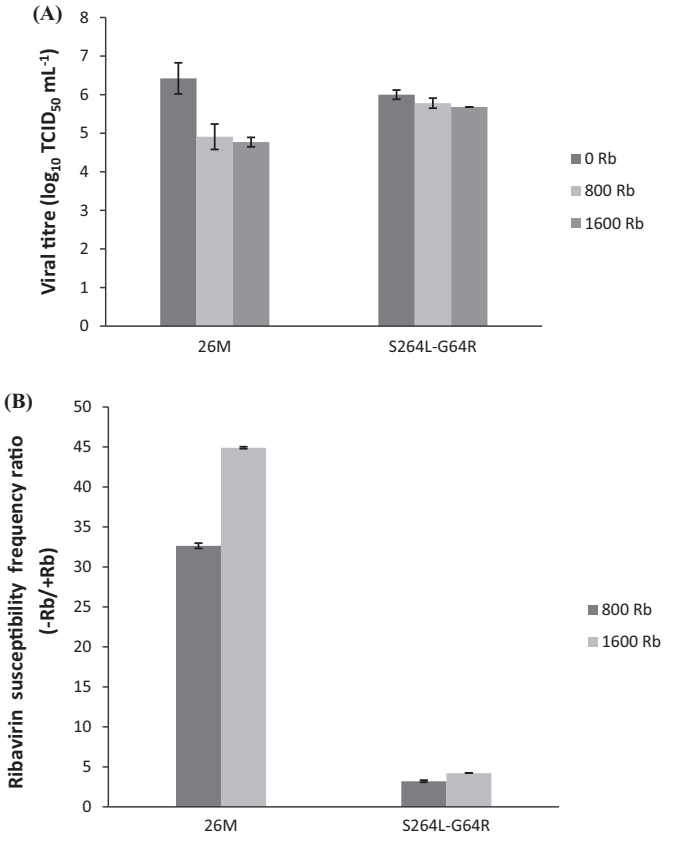

Fig. 1. Ribavirin resistance of S264L-G64R and parental 26M. (A) Titres of S264L-G64R and parental 26M (MOI = 0.1) after 24 h of growth in RD cells in the presence or absence of 800 μM or 1600 μM ribavirin (Rb). The resulting viral titres were determined by $TCID_{50}$ assay on Vero cells (Reed and Muench, 1938). The experiment was performed in triplicate and error bars indicate one standard error about the mean (SEM). (B) Ribavirin resistance frequency was calculated as the viral titre in absence of ribavirin (Rb) divided by the titre in the presence of ribavirin. The experiment was performed in triplicate and error bars indicate one standard error about the mean (SEM).

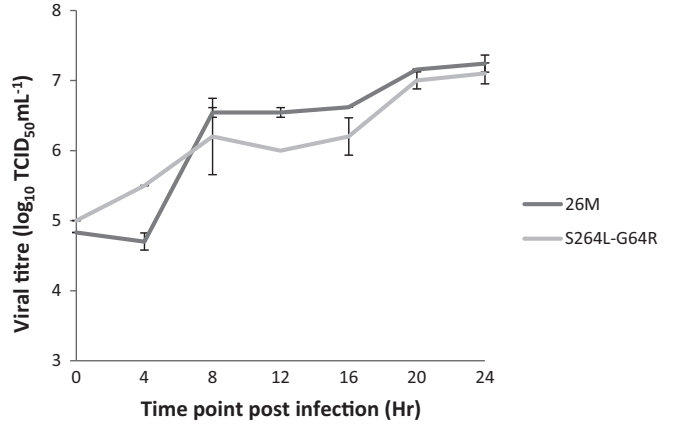

Fig. 2. Comparison of the single-step growth properties of S264L-G64R and 26M in RD cells. RD cell monolayers in 48-well tissue culture trays were infected with S264L-G64R or 26M (MOI = 10). Viruses were harvested at four hourly intervals for 24 h and yields were quantified by $TCID_{50}$ assay on Vero cells (Reed and Muench, 1938). The experiment was performed in triplicate and error bars indicate one standard error about the mean (SEM). The difference between the growth curves was assessed using one-way ANOVA and Tukey's multiple comparison tests. The difference in the single-step growth titres of the S264L-G64R and 26M populations were not found to be significant ($P > 0.05$). (Data were analysed using the GraphPad Prism online software package version 5.04 (http://www.graphpad.com).

3.4. Analysis of genome replication fidelity in a cloned population of S264L-G64R after passage in the presence of ribavirin

3.4.1. Development of guanidine resistance in S264L-G64R during passage in the presence of ribavirin

We previously developed a guanidine resistance assay to investigate the replication fidelity of the ribavirin-resistant G64R and S264L $3D^{pol}$ variant populations (Sadeghipour et al., 2013). Here, we report the use of this assay to compare the replication fidelity phenotype of S264L-G64R with parental 26M before and after serial passage in the presence of ribavirin.

In order to compare the frequency of the random accumulation of mutations within the genomes of parental 26M and S264L-G64R during passage in the presence of ribavirin, seven plaque-purified virus populations from independently derived stocks of S264L-G64R and 26M were passaged (×13) in RD cells in the presence of 400 μM ribavirin and the resistance to guanidine of the RD-passaged viral populations was determined at passage level thirteen.

The guanidine sensitivities of seven plaque-purified populations S264L-G64R and 26M after growth in RD cells for 48 h in the presence or absence of 0.5 mM guanidine are shown in Fig. 3. Plaque-purified 26M populations grew to higher titres in the presence of 0.5 mM guanidine (10–100-fold) compared to plaque-purified S264L-G64R populations (Fig. 3). These data suggest that cloned S264L-G64R populations have a higher viral RNA replication fidelity phenotype during growth in RD cells than parental virus, preventing the random selection of mutations in coding region 2C that confer the guanidine-resistant phenotype.

3.4.2. Nucleotide sequence analysis of the 2C and 3D coding regions of the S264L-G64R after passage in the presence of ribavirin

Genome mutation frequencies were estimated by nucleotide sequencing of the 2C and 3D coding regions of three randomly selected plaque-purified populations for each CDV – 26M1-3 and S264L-G64R1-3, respectively; a total of 8099 nucleotides was sequenced for each CDV. The mutation frequency of S264L-G64R mutant virus is represented as the average number of changes from parental 26M full-genome consensus sequence (7412 nucleotides). Parental 26M had acquired an average of 9.2 mutations per genome (7412 nucleotides) at RD passage 13. By contrast, the S264L-G64R had acquired an average of only 1.8 ($P < 0.0001$) mutations per genome, respectively. Our data indicate that S264L-G64R has a high replication fidelity phenotype, resulting in six-fold fewer mutations being introduced into HEV71 genome during passage in the presence of ribavirin (400 μM) compared to parental virus. This finding is consistent with our previous observations (Sadeghipour et al., 2013).

3.5. Construction of mouse-adapted variants of the high fidelity HEV71 $3D^{pol}$ variants

Given the association between increased replication fidelity of poliovirus and virulence in animal models (Vignuzzi et al., 2006, 2008), we decided to investigate the virulence of the HEV71 high replication fidelity variants in a mouse model of HEV71 infection (Chua et al., 2008). We previously showed that the major molecular determinant of HEV71 mouse adaptation and virulence is located in capsid protein VP1 (G145E) (Chua et al., 2008; Zaini and McMinn, 2012; Zaini et al., 2012). Furthermore, the mouse-adapted phenotype can be generated by the introduction of this mutation into the VP1 coding region of a parental HEV71 infectious cDNA clone (MP-26M) (Chua et al., 2008). In order to study the virulence of the HEV71 high replication fidelity variants in a mouse model, $3D^{pol}$ coding region cDNA fragments carrying the G64R, S264L

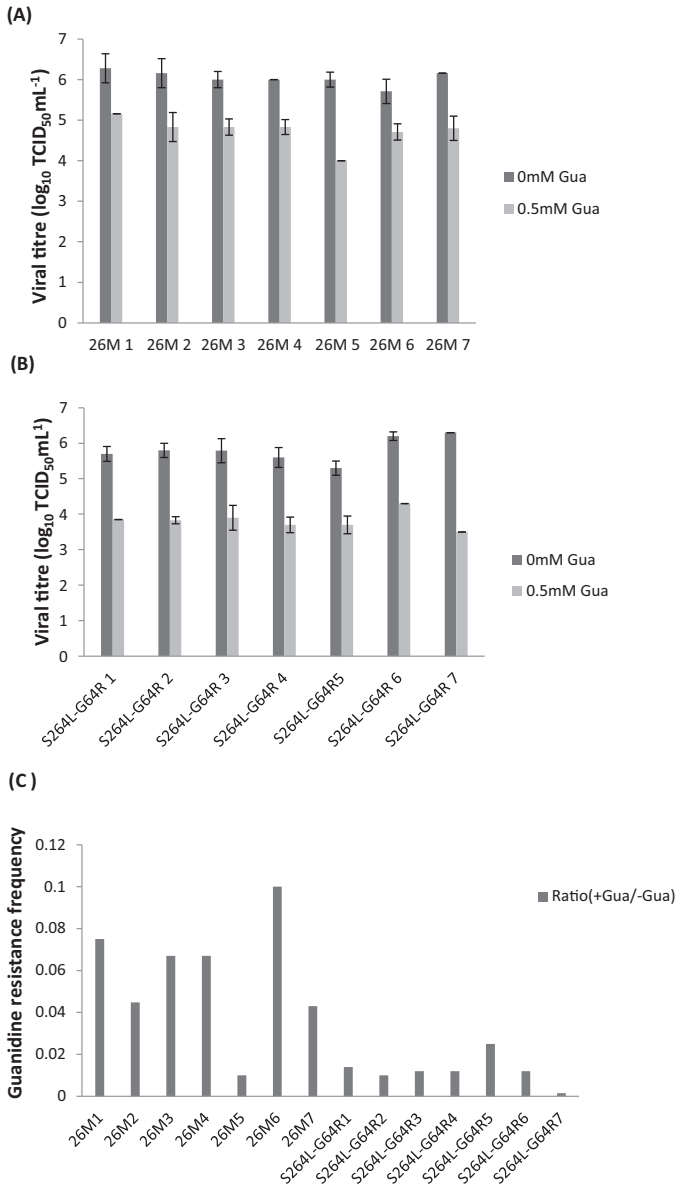

Fig. 3. Guanidine resistance of seven plaque-purified populations of S264L-G64R and parental 26M after passage in RD cells in the present of ribavirin. Seven plaque-purified populations of (A) 26M, and, (B) S264L-G64R, after 13 passages in the presence of ribavirin (400 μM), were cultured (MOI = 0.1) for 48 h in RD cells in the presence or absence of 0.5 mM guanidine (Gua). The resulting viral titres were determined by $TCID_{50}$ assay on Vero cells (Reed and Muench, 1938). The experiment was performed in triplicate and error bars indicate one standard error about the mean (SEM). (C) The guanidine resistance ratio of 26M and S264L-G64R was calculated as the viral titre in presence of guanidine divided by the titre in the absence of guanidine, based on the final titres shown in Fig. 2A and B. The experiment was performed in triplicate and error bars indicate one SEM.

or S264L-G64R mutations were cloned into MP-26M, generating the mouse-adapted variants MP-G64R, MP-S264L and MP-S264L-G64R, respectively. The VP1 coding region of the mouse-adapted CDVs was amplified by RT-PCR after one passage in RD cells and sequenced to confirm the presence of mouse adaptation marker (G145E) in the rescued CDV populations (data not shown).

3.6. Susceptibility of BALB/c mice to infection with MP-G64R, MP-S264L, MP-S264L-G64R and MP-26M

Next we characterised the virulence of MP-G64R, MP-S264L, MP-S264L-G64R and MP-26M in mice. Groups of six 5-day-old BALB/c mice were infected i.p. with $5 \times TCID_{50}$, $50 \times TCID_{50}$, $5 \times 10^2 \times TCID_{50}$, $5 \times 10^3 \times TCID_{50}$ or $5 \times 10^4 \times TCID_{50}$ of MP-26M, MP-G64R, MP-S264L or MP-S264L-G64R, respectively, and the results are shown in Table 1. Mice were monitored twice daily for 14 days post-infection (p.i.) and the percentage survival was calculated for each group. Mice infected with $5 \times 10^3 \times TCID_{50}$ or $5 \times 10^4 \times TCID_{50}$ of MP-26M, MP-G64R, MP-S264L or MP-S264L-G64R showed similar clinical signs of infection, including forelimb and/or hind limb flaccid paralysis, ruffled fur, weight loss and severe lethargy. Infected mice were euthanised upon reaching clinical grade 3 paralysis (hunched posture, flaccid paralysis). The HD_{50} values of MP-26M, MP-G64R, MP-S264L and MP-S264L-G64R infection in newborn BALB/c mice are 5×10^3 $TCID_{50}$, 8.5×10^3 $TCID_{50}$, 1.6×10^4 $TCID_{50}$ and 1.6×10^4 $TCID_{50}$, respectively. Significant differences in HD_{50} values were observed between parental MP-26M and MP-S264L ($P < 0.05$) and between parental MP-26M and MP-S264L-G64R ($P < 0.05$). By contrast, no difference was observed in HD_{50} values between parental MP-26M and MP-G64R.

Table 1
Survival of 5-day-old BALB/c mice infected by i.p. inoculation with ten-fold serial dilutions of MP-26M, MP-G64R, MP-S264L and MP-S264L-G64R.

Virus	Dose ($TCID_{50}$)	Survival[a]
MP-26M	5×10^0	6/6
	5×10^1	6/6
	5×10^2	5/6
	5×10^3	3/6
	5×10^4	0/6
MP-G64R	5×10^0	6/6
	5×10^1	6/6
	5×10^2	5/6
	5×10^3	4/6
	5×10^4	0/6
MP-S264L	5×10^0	6/6
	5×10^1	6/6
	5×10^2	6/6
	5×10^3	5/6
	5×10^4	1/6
MP-S264L-G64R	5×10^0	6/6
	5×10^1	6/6
	5×10^2	6/6
	5×10^3	5/6
	5×10^4	1/6
Mock-infected	–	6/6

[a] The number of mice surviving in groups of six mice.

The mean survival time of mice infected with 5×10^4 $TCID_{50}$ of parental MP-26M was 6.0 (±0.0) days; the mean survival time of mice infected with 5×10^4 $TCID_{50}$ of MP-G64R was 6.5 (±1.41) days; the mean survival time of mice infected with 5×10^4 $TCID_{50}$ of MP-S264L was 7.0 (±0.0) days; and the mean survival time of mice infected with 5×10^4 $TCID_{50}$ of MP-S264L-G64R was 7.5 (±1.41) days. MP-S264L- and MP-S264L-G64R-infected mice survived significantly ($P < 0.05$) longer than MP-26M-infected mice. Moreover, the average survival of MP-G64R-infected mice did not differ from mice infected with MP-26M ($P > 0.05$).

3.7. Tissue distribution of MP-G64R, MP-S264L, MP-S264L-G64R and MP-26M in BALB/c mice

Next we investigated the tissue distribution of MP-G64R, MP-S264L, MP-S264L-G64R and MP-26M after i.p. inoculation of newborn BALB/c mice. Groups of nine 5-day-old BALB/c mice were infected or mock-infected i.p. with $50 \times HD_{50}$ of MP-G64R, MP-S264L, MP-S264L-G64R or MP-26M.

In MP-26M-infected mice, virus was first detected in the blood (3.4×10^2 $TCID_{50}$/mL) and in skeletal muscle (4.5×10^5 $TCID_{50}$/g) at three days p.i. (Fig. 4). At five days p.i., MP-26M was present in blood

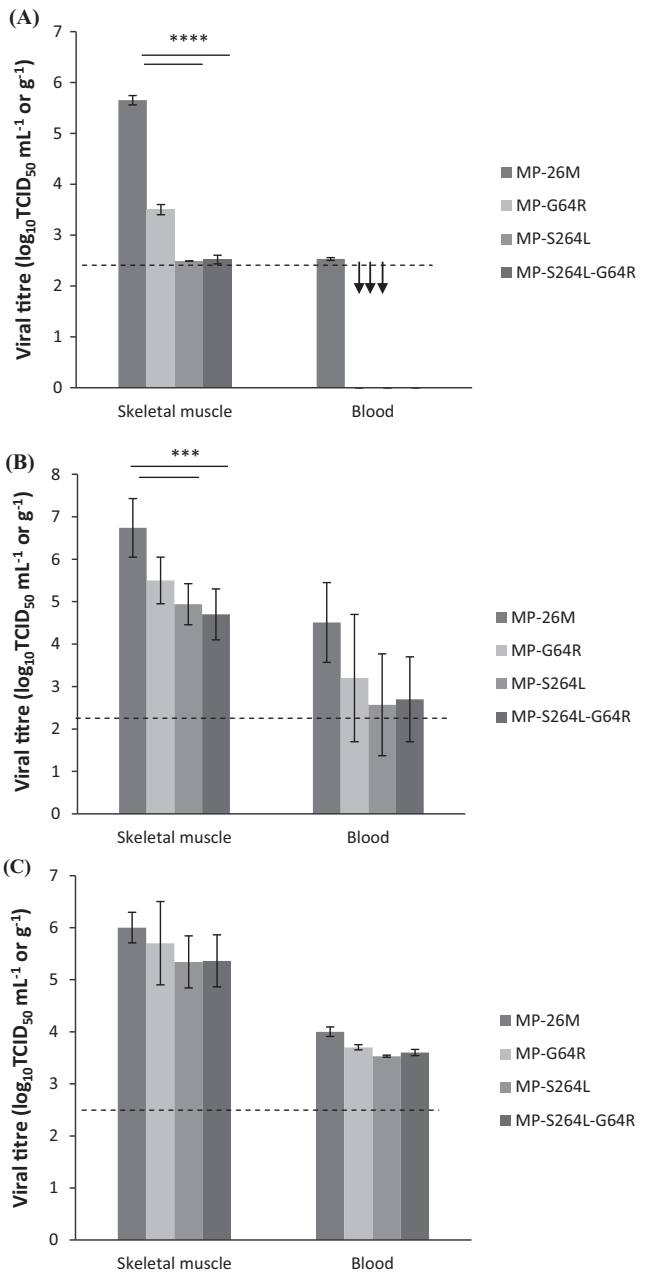

Fig. 4. Viral loads in selected tissues of 5-day-old BALB/c mice after i.p. challenge with $50 \times HD_{50}$ of MP-26M, MP-G64R, MP-S264L or MP-S264L-G64R at (A) three days p.i., (B) five days p.i., and, (C) six days p.i. Viral titres in blood were determined as $TCID_{50}$ mL^{-1} and viral titres in skeletal muscle homogenates were determined as $TCID_{50}$ g^{-1}. Each time-point represents the mean tissue titre in three mice; error bars represent one standard error about the mean (SEM). The limit of detection (LoD) of virus titration by $TCID_{50}$ assay is $2.2 \times \log_{10}$ $TCID_{50}$. The dashed line indicates the LoD of virus titration by $TCID_{50}$; arrows indicate specimens with titres below the LoD. Significant differences were observed in skeletal muscle growth titres between parental MP-26M and MP-S264L at both three (****$P < 0.0001$) and five (***$P < 0.001$) days p.i. Significant differences were also observed in skeletal muscle growth titres between parental MP-26M and MP-S264L-G64R at both three (****$P < 0.0001$) and five (***$P < 0.001$) days p.i.

(3.2×10^4 $TCID_{50}$/mL) and in skeletal muscle (5.5×10^6 $TCID_{50}$/g). The high skeletal muscle tissue titres in MP-26M-infected mice are consistent with our previous observations (Chua et al., 2008). In MP-G64R-infected mice, virus was first detected in the skeletal muscle (3.2×10^3 $TCID_{50}$/g) at three days p.i. At five days p.i., MP-G64R was detected in blood (1.6×10^3 $TCID_{50}$/mL) and skeletal muscle (3.2×10^5 $TCID_{50}$/g). No significant differences in growth titres were observed in the tissues of MP-26M- and MP-G64R-infected mice (Fig. 4). In MP-S264L-infected mice, virus was first detected at three days p.i. in skeletal muscle (3.1×10^2 $TCID_{50}$/g). At five days p.i., MP-S264L was detected in blood (5.1×10^2 $TCID_{50}$/mL) and skeletal muscle (1.0×10^6 $TCID_{50}$/g). Similarly, in MP-S264L-G64R-infected mice, virus was first detected at three days p.i. in skeletal muscle (3.3×10^2 $TCID_{50}$/g). At five days p.i., MP-S264L-G64R was detected in blood (5.0×10^2 $TCID_{50}$/mL) and skeletal muscle (5.5×10^6 $TCID_{50}$/g). It is interesting to note that viraemia titres of MP-26M-, MP-G64R-, MP-S264L and MP-S264L-G64R-infected mice were more variable at five days p.i. compared to six days p.i. Statistically significant differences in skeletal muscle growth titres were observed between MP-26M and MP-S264L and between MP-26M and S264L-G64R at both three ($P < 0.0001$) and five ($P < 0.001$) days p.i.

Taken together, these findings indicate that MP-S264L and MP-S264L-G64R have an attenuated virulence phenotype in mice, in which the delayed onset of clinically-apparent disease is associated with lower viral titres in skeletal muscle and with the delayed onset of necrotising skeletal muscle myositis (see below).

3.8. Histological analysis of MP-G64R-, MP-S264L-, MP-S264L-G64R- and MP-26M-infected tissues

Histological studies were performed in order to determine if the differences in viral growth in MP-26M-, MP-G64R- and MP-S264L- or MP-S264L-G64R-infected mice were associated with differing tissue pathologies. Groups of three 5-day-old BALB/c mice were inoculated i.p. with $50 \times HD_{50}$ of MP-G64R, MP-S264L, MP-S264L-G64R or MP-26M.

Histopathological changes observed in skeletal muscle tissue of MP-26M-and $3D^{pol}$ variant-infected mice are shown in Fig. 5. No histological abnormalities were observed in the skeletal muscle of age-equivalent mock-infected mice (Fig. 5A). At five days p.i., severe necrotising myositis was observed in MP-26M-infected mice (Fig. 5B) and in MP-G64R-infected mice (Fig. 5C). By contrast, mild focal myositis was observed in MP-S264L-infected mice (Fig. 5D) and in MP-S264L-G64R-infected mice (Fig. 5E) at five days p.i. The histological data are consistent with the findings of the tissue distribution analysis (Fig. 4), in which high-titre skeletal muscle infection was observed in MP-26M- and MP-G64R-infected mice at three days p.i, whereas high titre skeletal muscle infection of MP-S264L- and MP-S264L-G64R-infected mice was delayed until five days p.i.

4. Discussion

Poliovirus strains expressing mutations at position G64 in $3D^{pol}$ have a high replication fidelity phenotype and are attenuated in poliovirus receptor-expressing transgenic mice (Pfeiffer and Kirkegaard, 2005; Vignuzzi et al., 2006, 2008). We recently extended this observation to HEV71 by demonstrating that two mutations (G64R, S264L) in the HEV71 $3D^{pol}$ generate a high replication fidelity phenotype and restrict genomic diversity (Sadeghipour et al., 2013). Therefore, in this study, we were interested to determine if these $3D^{pol}$ mutations also attenuate the virulence of HEV71. Prior to undertaking virulence studies in mice, we constructed a HEV71 strain that incorporates both $3D^{pol}$ mutations (S264L plus G64R). The double mutant CDV (S264L-G64R) was ribavirin resistant and had a six-fold higher replication fidelity phenotype than parental virus, as we have previously shown for HEV71 strains incorporating single $3D^{pol}$ mutations (Sadeghipour et al., 2013). Furthermore, the $3D^{pol}$ mutations did not alter the replicative capacity of S264L-G64R in RD cell culture.

In this study, we have shown that S264L and S264L-G64R are attenuated in mice. Clinically-apparent disease was significantly

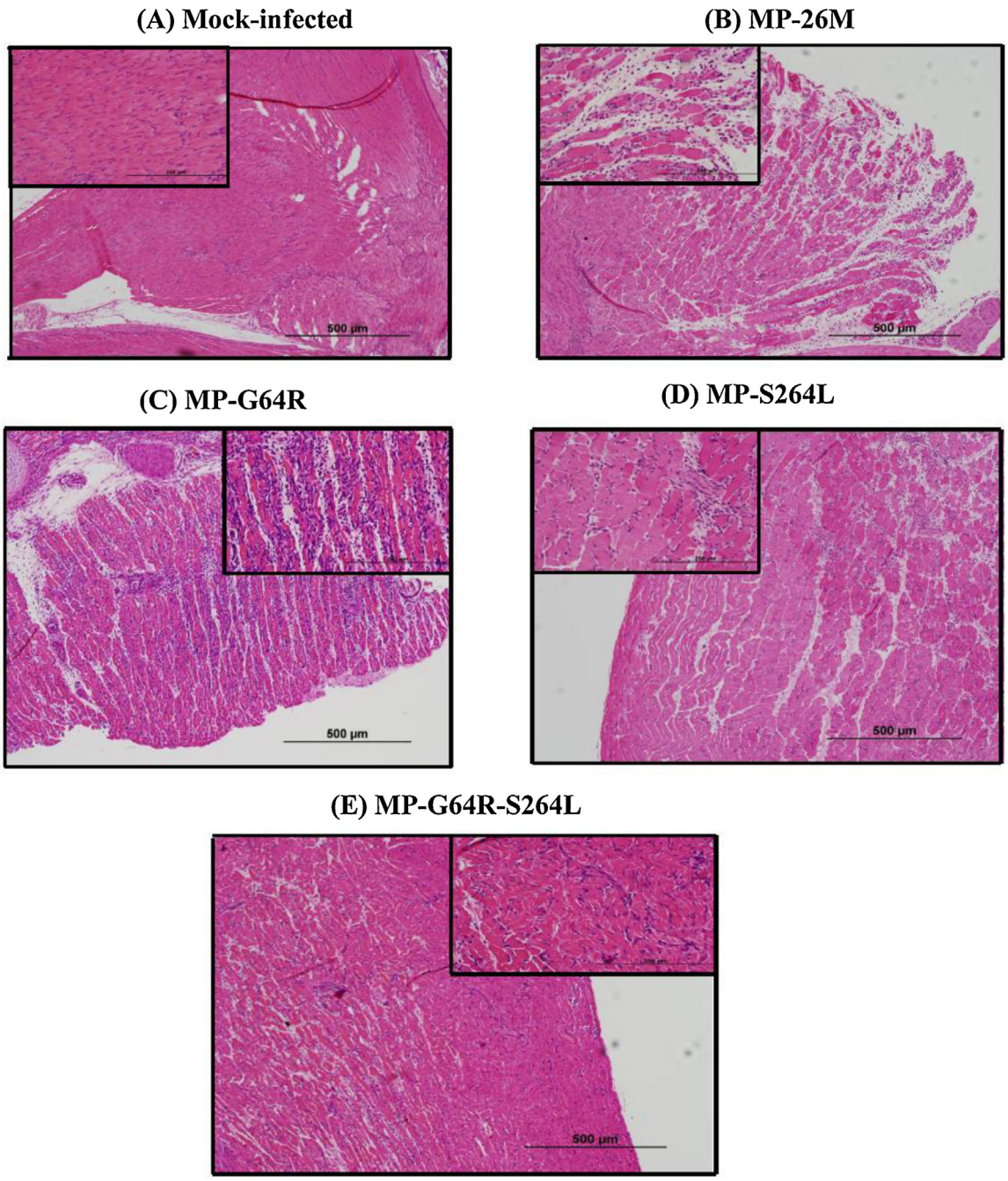

Fig. 5. Histological analysis of skeletal muscle in MP-26M-, MP-G64R-, MP-S264L-, and MP-S264L-G64R-infected, 5-day-old BALB/c mice. Groups of three 5-day-old BALB/c mice were mock-infected (A) or infected with 50 × HD_{50} of MP-26M (B), MP-G64R (C), MP-S264L (D) or MP-S264L-G64 (E). Skeletal muscle tissue was collected from mice at 5 days p.i., fixed in 10% buffered formalin overnight, dehydrated in 70% ethanol and embedded in paraffin. For each tissue specimen, several sections (4–5 μm) were cut with a microtome, mounted onto glass slides (VWR Labware) and stained with haematoxylin and eosin. Tissue sections were examined at 10 × magnification and at 40× magnification (inset); bars indicate length in μm.

delayed and was associated with lower viral titres in skeletal muscle and with the delayed onset of necrotising skeletal muscle myositis. By contrast, G64R was not attenuated in mice and had a similar virulence phenotype to parental virus, suggesting that high replication fidelity may not be the sole determinant of virulence attenuation of mouse-adapted HEV71. However, it should be noted that G64R titres in the blood and skeletal muscle tissues of infected mice were significantly lower than in mice infected with parental virus, especially on days 3 and 5 post-infection. This suggests that the G64R mutation may have impacted negatively on viral fitness *in vivo* without leading to a measurable decrease in virulence in newborn BALB/c mice.

Two alternative explanations for our inability to identify virulence attenuation in G64R are worth noting. Firstly, the inherent insensitivity of our newborn mouse model of HEV71 infection may have prevented the detection of attenuation due to the 3D-G64R mutation. Secondly, it is possible that ribavirin mutagenesis may have induced virulence attenuation of HEV71 *via* a differential effect on quasispecies diversity and the fitness of the S264L and G64R populations, as reported by Sanz-Ramos et al. (2012).

The association between the ribavirin resistance, replication fidelity and viral virulence phenotypes is complex. As previously noted, a high replication fidelity strain of poliovirus (3D-G64S)

is attenuated in mice (Pfeiffer and Kirkegaard, 2005; Vignuzzi et al., 2006, 2008). Furthermore, Castro et al. (2009) identified a conserved lysine residue that contributes to the catalytic efficiency and copying fidelity of all nucleic acid polymerases; mutation of this lysine residue to arginine (K359R) in the poliovirus $3D^{pol}$ generated a virus population that had a higher replication fidelity phenotype and was more highly attenuated in mice than the G64S variant (Weeks et al., 2012). Similarly, mutations in the alphavirus chikungunya RNA-dependent RNA polymerase that increase replication fidelity and decrease genome diversity also impact negatively on viral fitness in both vertebrate and invertebrate hosts (Coffey and Vignuzzi, 2011). Interestingly, mutations in the Coxsackievirus B3 $3D^{pol}$ coding region that generate a low replication fidelity phenotype and increased genome diversity also attenuate virulence in mice (Gnädig et al., 2012). Furthermore, a strain of SARS coronavirus (SARS-CoV) engineered to express low replication fidelity (inactivation $3' \rightarrow 5'$ exonuclease activity) is stably attenuated in mice (Graham et al., 2012).

Sanz-Ramos et al. (2012) reported that a ribavirin mutagenised foot-and-mouth disease virus (FMDV) population was attenuated in mice even though a large proportion of clones within the quasispecies were highly virulent. Furthermore, a 2C-I248T mutation that was associated with the attenuated FMDV population did not attenuate wild type virus when incorporated into an infectious clone (Sanz-Ramos et al., 2008). Sanz-Ramos et al. (2012) further demonstrated that mixed wild-type and ribavirin-mutagenised FMDV populations were attenuated in mice, suggesting that the mutagenised quasispecies population exerted a suppressive effect on virulence. Genome length sequence analysis and mixed viral population virulence studies of ribavirin-mutagenised HEV71 would enable us to determine if this mechanism also contributes to the attenuated phenotype of S264L.

The mouse model used in this study (Chua et al., 2008) requires prior adaptation of virus and thus the inability to identify virulence attenuation in 3D-G64R-expressing HEV71 strains may result from the inherent insensitivity of this model. Studies in the cynomolgus macaque model (Nagata et al., 2002) would assist in the investigation of the link between replication fidelity and virulence attenuation of HEV71. Poliovirus receptor-expressing transgenic mice provide a more authentic model for the investigation of enterovirus virulence (Ren et al., 1990) than mouse adaptation. Two human receptors for HEV71, scavenger receptor B2 (Yamayoshi et al., 2009) and p-selectin glycoprotein ligand-1 (Nishimura et al., 2009), have recently been identified. However, a recent study has shown that p-selectin glycoprotein ligand-1 transgenic mice are not susceptible to HEV71 infection (Liu et al., 2012). Thus, the development of transgenic mice expressing scavenger receptor B2 may be required to provide a more authentic mouse model for the investigation of HEV71 virulence.

In conclusion, we have shown that the 3D-S264L mutation, which confers high replication fidelity upon HEV71, attenuates the virulence of HEV71 in newborn BALB/c mice. By contrast, the 3D-G64R mutation, which also confers high replication fidelity upon HEV71, does not attenuate HEV71. Although this suggests that a high replication fidelity phenotype is not directly responsible for virulence attenuation in this model, further studies of ribavirin-mutagenised HEV71 populations and the use a more authentic animal model of HEV71 infection are required to clarify this issue. Nevertheless, as more information emerges on the molecular processes involved in HEV71 infection and virulence, a clearer picture will emerge of the major determinants of HEV71 virulence and of the association between replication fidelity and virulence. Finally, the information obtained in this study is of potential use in the development of a live attenuated vaccine to protect against HEV71 encephalitis in young children.

Acknowledgments

We thank Ms Emily Bek for expert technical assistance.

References

Castro, C., Smidansky, E.D., Arnold, J.J., Maksimchuk, K.R., Moustafa, I., Uchida, A., Gotte, M., Konigsburg, W., Cameron, C.E., 2009. Nucleic acid polymerases use a general acid for nucleotidyl transfer. Nature Structural Biology 16 (2), 212–218.

Chua, B.H., Phuektes, P., Sanders, S.A., Nicholls, P.K., McMinn, P.C., 2008. The molecular basis of mouse adaptation by human enterovirus 71. Journal of General Virology 89 (7), 1622–1632.

Coffey, L.L., Vignuzzi, M., 2011. Host alternation of chikungunya virus increases fitness while restricting population diversity and adaptability to novel selective pressures. Journal of Virology 85 (2), 1025–1035.

Gnädig, N.F., Beaucourt, S., Campagnola, G., Bordería, A.V., Sanz-Ramos, M., Gong, P., Blanc, H., Peersen, O.B., Vignuzzi, M., 2012. Coxsackievirus B3 mutator strains are attenuated in vivo. Proceedings of the National Academy of Sciences 109 (34), E2294–E2303.

Graham, R., Becker, M., Eckerle, L., Bolles, M., Denison, M., Baric, R., 2012. A live, impaired-fidelity coronavirus vaccine protects in an aged, immunocompromised mouse model of lethal disease. Nature Medicine 18 (12), 1820–1826.

Knowles, N.J., Hovi, T., Hyypiä, T., King, A.M.Q., Lindberg, A.M., allansch, M.A., Palmenberg, A.C., immonds, P., kern, T., Stanway, G., Yamashita, T., Zell, R., 2012. Picornaviridae. In: Virus Taxonomy: Classification and Nomenclature of Viruses. Elsevier, San Diego.

Liu, J., Dong, W., Quan, X., Ma, C., Qin, C., Zhang, L., 2012. Transgenic expression of human P-selectin glycoprotein ligand-1 is not sufficient for enterovirus 71 infection in mice. Archives of Virology 157 (3), 539–543.

McMinn, P., 2002. An overview of the evolution of enterovirus 71 and its clinical and public health significance. FEMS Microbiology Review 26 (1), 91–107.

McMinn, P., Stratov, I., Nagarajan, L., Davis, S., 2001. Neurological manifestations of enterovirus 71 infection in children during an outbreak of hand, foot, and mouth disease in western Australia. Clinical Infectious Diseases 32 (2), 236–242.

Nagata, N., Shimizu, H., Ami, Y., Tano, Y., Harashima, A., Suzaki, Y., Sato, Y., Miyamura, T., Sata, T., Iwasaki, T., 2002. Pyramidal and extrapyramidal involvement in experimental infection of cynomolgus monkeys with enterovirus 71. Journal of Medical Virology 67 (2), 207–216.

Nishimura, Y., Shimojima, M., Tano, Y., Miyamura, T., Wakita, T., Shimizu, H., 2009. Human P-selectin glycoprotein ligand-1 is a functional receptor for enterovirus 71. Nature Medicine 15 (7), 794–797.

Pfeiffer, J.K., Kirkegaard, K., 2003. A single mutation in poliovirus RNA-dependent RNA polymerase confers resistance to mutagenic nucleotide analogs via increased fidelity. Proceedings of the National Academy of Sciences 100 (12), 7289–7294.

Pfeiffer, J.K., Kirkegaard, K., 2005. Increased fidelity reduces poliovirus fitness and virulence under selective pressure in mice. PLoS Pathogens 1 (2), e11.

Reed, L.J., Muench, H., 1938. A simple method of estimating fifty per cent endpoints. American Journal of Epidemiology 27 (3), 493–497.

Ren, R., Costantini, F., Gorgacz, E.J., Lee, J.J., Racaniello, V.R., 1990. Transgenic mice expressing a human poliovirus receptor: a new model for poliomyelitis. Cell 63 (2), 353–362.

Sadeghipour, S., Bek, E.J., McMinn, P.C., 2013. Ribavirin-resistant mutants of human enterovirus 71 express a high replication fidelity phenotype during growth in cell culture. Journal of Virology 87 (3), 1759–1769.

Sanz-Ramos, M., Díaz-San Segundo, F., Escarmís, C., Domingo, E., Sevilla, N., 2008. Hidden virulence determinants in a viral quasispecies in vivo. Journal of Virology 82 (21), 10465–10476.

Sanz-Ramos, M., Rodríguez-Calvo, T., Sevilla, N., 2012. Mutagenesis-mediated decrease of pathogenicity as a feature of the mutant spectrum of a viral population. PLoS ONE 7 (6), e39941.

Vignuzzi, M., Stone, J.K., Arnold, J.J., Cameron, C.E., Andino, R., 2006. Quasispecies diversity determines pathogenesis through cooperative interactions in a viral population. Nature 439 (7074), 344–348.

Vignuzzi, M., Wendt, E., Andino, R., 2008. Engineering attenuated virus vaccines by controlling replication fidelity. Nature Medicine 14 (2), 154–161.

Weeks, S.A., Lee, C.A., Zhao, Y., Smidansky, E.D., August, A., Arnold, J.J., Cameron, C.E., 2012. A polymerase mechanism-based strategy for viral attenuation and vaccine development. Journal of Biological Chemistry 287 (38), 31618–31622.

Wright, A.J., Phillpotts, R.J., 1998. Humane endpoints are an objective measure of morbidity in Venezuelan encephalomyelitis virus infection of mice. Archives of Virology 143 (6), 1155–1162.

Yamayoshi, S., Yamashita, Y., Li, J., Hanagata, N., Minowa, T., Takemura, T., Koike, S., 2009. Scavenger receptor B2 is a cellular receptor for enterovirus 71. Nature Medicine 15 (7), 798–801.

Zaini, Z., McMinn, P., 2012. A single mutation in capsid protein VP1 (Q145E) of a genogroup C4 strain of human enterovirus 71 generates a mouse-virulent phenotype. Journal of General Virology 93 (Pt 9), 1935–1940.

Zaini, Z., Phuektes, P., McMinn, P., 2012. Mouse adaptation of a sub-genogroup B5 strain of human enterovirus 71 is associated with a novel lysine to glutamic acid substitution at position 244 in protein VP1. Virus Research 167 (1), 86–96.